

# Study of Parrondo's paradox regions in one-dimensional quantum walks

Munsif Jan,<sup>1,2</sup> Xiao-Ye Xu,<sup>1,2,\*</sup> Qin-Qin Wang,<sup>1,2</sup> Wei-Wei Pan,<sup>1,2</sup>  
Yong-Jian Han,<sup>1,2</sup> Chuan-Feng Li,<sup>1,2,†</sup> and Guang-Can Guo<sup>1,2</sup>

<sup>1</sup>CAS Key Laboratory of Quantum Information, University of Science and Technology of China, Hefei, 230026, China

<sup>2</sup>CAS Center For Excellence in Quantum Information and Quantum Physics,

University of Science and Technology of China, Hefei 230026, People's Republic of China

(Dated: July 1, 2020)

The well-known counterintuitive phenomenon, where the combination of unfavorable situations can establish favorable ones, is called Parrondo's paradox. Here, we study one-dimensional discrete-time quantum walks, manipulating two different coins (two-state) operators representing two losing games A and B, respectively, to create the Parrondo effect in the quantum domain. We exhibit that game A and B are losing games when played individually but could produce a winning expectation when played alternatively for a particular sequence of the different periods. Moreover, we also analyze the relationships between Parrondo's games and quantum entanglement in our scheme. Along with the applications of different kinds of quantum walks, our outcomes potentially encourage the development of new quantum algorithms.

Parrondo's paradox, which was originally based on flashing Brownian ratchet [1, 2], characterizes counterintuitive gambling games where two individually losing games can construct a winning game when combined in a right way [3, 4]. The original Parrondo's paradox have two versions, referred as capital-dependent [3–5] and history-dependent [2, 6]. The only difference between these two versions is just the switching mechanism of game B. These paradoxical mechanism has been observed in many situations of interest, for example, counterintuitive drift in the physics of granular flow [7], enzyme transport analyzed by a four-state rate mode [8], combination of declining branching processes produces an increase [9], and finance model where capital increases by investing an assets with negative growth rate [10]. In the last two decades, the Parrondo's paradox has been extended to various fields ranging from physics [11–18], population genetics [19–21], and even to economics [22], which has attracted a particular attention due to its potential to characterize the strategy of altering the unstable situation into a stable ones. Although the paradox has been proposed theoretically in the classical and quantum systems [11, 12, 16–18], the experimental realization of the quantum version of the effect is still unfulfilled, to the best of our knowledge. It is well-known that the classical Parrondo effect is a type of random walk that can be described by the Fokker-Planck equation [23]; and it is also known that the Fokker-Planck equation is a Wick rotation of the Schrödinger equation [24], thus there are deep interconnections between these types of classical random walks and quantum walks. Our work motivates the future exploration of these ideas.

Quantum walks (QWs) [25, 26], which are natural extensions of the classical random walks (CRWs) in the quantum domain, that possess a quadratic gain over the

CRWs [27] due to the remarkable features like interference and superposition. Thus, QWs offer a flexible and powerful platform to investigate different physics, ranging from the design of efficient algorithms in quantum information processing [28–30] (even constructing universal quantum computation [31, 32]), the realization of exotic physical phenomena in the context of topological phases [33–35], to quantum physics out of equilibrium [36] (for example, observing the dynamical quantum phase transition [37–39] and even investigating quantum thermodynamics [40–44]). The Parrondo effect in the quantum walks has been proposed in [45–50], using different strategies and it can also be viewed as a special sample of the disordered QWs [51, 52]. The periodic sequence and dynamic disorder QWs, which possess some distinctive properties, such as, it can help to enhance the entanglement between the coin and the position [53–55]. Unlike the CRWs, QWs are characterized by quantum superpositions of amplitudes rather than classical probability distributions. However, the coherent character of the QW plays a vital role in the realization of a quantum Parrondo game. Recently, we have experimentally realized the quantum version of Parrondo effect [56], based on our currently developed compact large-scale QW platform [57].

Here, we demonstrate the genuine quantum Parrondo effect in 1-D discrete time QWs using two different coins operations, i.e.,  $C_A$  and  $C_B$ , representing game A and B, respectively. We show that game A and B are individually losing games, but when we play these two games alternatively in the particular sequence of different periods, could produce a winning game which is known as Parrondo's paradox. Recent attempts [47, 48, 50] have been failed to realize the true Parrondo game in QWs for the case of a two-state coin (qubit) over the infinite steps. Decohering QW by introducing a pure dephasing channel can disappear the quantum Parrondo effect [56], indicates that coherence plays a key role in the emergence of the quantum Parrondo effect. In addition, we also discuss the relationship between quantum Parrondo's games

\* xuxiaoye@ustc.edu.cn

† cffi@ustc.edu.cn

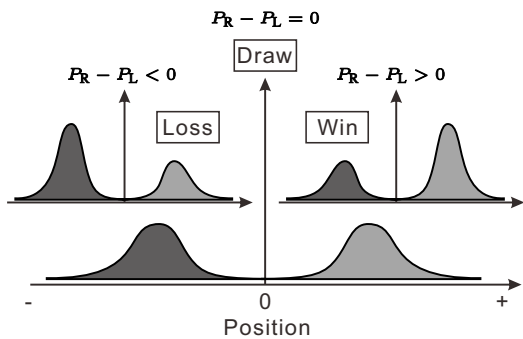


FIG. 1. An illustration of a winning versus a losing strategy in a 1-D QW. Black and grey distributions show the probabilities of the walker to the left  $P_L$  and right  $P_R$  of the origin, respectively.

and coin-position entanglement in our scenario.

We suppose one-dimensional (1-D) discrete-time QWs whose total Hilbert space can be expressed as  $H = H_c \otimes H_p$ , where  $H_c$  is a two-dimensional coin space spanned by  $\{|0\rangle, |1\rangle\}$ , and  $H_p$  represents an infinite-dimensional site space spanned by  $|x\rangle$  ( $x \in Z$  is the site). Each step of the QW possesses two operations  $C$  and  $S$ :  $C$  is the rotation of coin state in  $H_c$ , and  $S$  is the shift operator which describes the movement of the walker according to the coin state. Generally, the coin rotation operator of a two-dimensional space is defined by three parameters  $(\alpha, \beta, \gamma)$ , i.e

$$C(\alpha, \beta, \gamma) = \begin{pmatrix} e^{i\alpha} \cos \beta & -e^{-i\gamma} \sin \beta \\ e^{i\gamma} \sin \beta & e^{-i\alpha} \cos \beta \end{pmatrix}. \quad (1)$$

Different rotation operators describe distinct QWs correspond to different games. The shift operator can be defined as

$$S = \sum_{x=-\infty}^{\infty} (|0\rangle\langle 0| \otimes |x+1\rangle_p \langle x|_p + |1\rangle\langle 1| \otimes |x-1\rangle_p \langle x|_p). \quad (2)$$

Therefore, the single step evolution of the QW can be described as:  $U = S \cdot C(\alpha, \beta, \gamma)$ . In our scheme, the generic unbiased initial state of the walker is prepared as  $|\Psi(0)\rangle = \frac{1}{\sqrt{2}}(|0\rangle + e^{i\eta}|1\rangle)_c \otimes |x\rangle_p$ , where the subscript  $c$ , ( $p$ ) represents the coin (position) state, respectively. The global state at time step  $t$  ( $t$  is an integer) then read as  $|\Psi(t)\rangle = U^t |\Psi_0\rangle$ .

To demonstrate the paradoxical scenario of Parrondo game in a 1-D discrete-time QW, we define a game on the state  $\Psi(t)$ . Note that we can use the bias of the probability distribution of  $\Psi(t)$  to define the state of winning and losing outcome of the game. The winning and losing of game can be decided according to the strategy shown in Fig. 1: if  $P_R - P_L > 0$  ( $P_L = \sum_{x=-\infty}^{-1} |\langle x|\Psi(t)\rangle|^2$  and  $P_R = \sum_{x=1}^{\infty} |\langle x|\Psi(t)\rangle|^2$ ), which means that the walker has a greater probability of appearing at the right of the origin, represents a winning game; on the contradictory,

if  $P_R - P_L < 0$ , the game is losing; when  $P_R = P_L$ , this represents a draw situation. If  $P_R - P_L > 0$  is maintained throughout the dynamics, it indicates a winning expectation of the game. Similarly, the converse situation denotes a losing expectation as shown in Fig. 1.

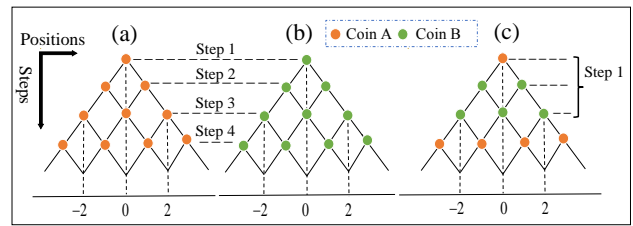


FIG. 2. (Color online) An illustration of a coin operation in a 1-D QW for (a) game A realized with  $C_A$  (orange), (b) game B realized with  $C_B$  (green), and (c) game ABB played with both coins in the periodic sequence of  $C_A C_B C_B$ , respectively.

Here, as an example, we discuss three different regions where we play game A with coin rotation operator  $C_A$  (orange) and game B with operator  $C_B$  (dark grey), as shown in the Fig. 2(a) and (b), respectively. We exhibit that in all regions when playing game A and B individually at any time,  $t$  will lose the game according to the definition. However, when we play these two games alternatively for a particular sequence of different periods, i.e., among which we have only sketched the coin operation pattern for game ABB (that is, we use one-time  $C_A$  and two-time  $C_B$  for every single step) as shown in the Fig. 2(c), can create a winning expectation all the time, which is known as Parrondo's paradox.

Firstly, we investigate the dynamics of probability distribution in 1-D discrete-time QWs corresponding to game A and B individually. In the game A(B), the quantum state at the step  $t$  is  $|\Psi(t)\rangle_{A(B)} = (S \cdot C_{A(B)})^t |\Psi(0)\rangle$ . The simulation results of the bias of the distribution of the states  $\Psi_{A(B)}(t)$ , i.e.,  $P_R(t) - P_L(t)$  for game A and B, are illustrated in Fig. 3: Fig. 3(a) corresponding to the game A with rotation operator  $C_A = C(150, 30, 172)$  and game B with rotation operator  $C_B = R(175, 65, 165)$ . It is clear that both game A and game B are losing games and the bias distribution  $P_R - P_L$  are negative throughout the number of steps  $t$ . Whenever we play game A and B alternatively for the particular sequence of different periods, e.g., the game ABB, rotating the coins in the sequence of  $C_A C_B C_B$  which has a period of 3 as shown in Fig. 2(c), one can observe some counterintuitive behavior. In this scenario the quantum state at step  $t$  is  $|\Psi(t)\rangle_{ABB} = (S \cdot C_B \cdot S \cdot C_B \cdot S \cdot C_A)^t |\Psi(0)\rangle$ , the simulation results of the bias distribution of the state at any step  $t$  are depicted in Fig. 3(b). Similarly, one can also see the same counterintuitive behavior for the the sequence of BBAA with coin rotation  $C_B C_B C_A C_A$  and BBAAA with coin rotation  $C_B C_B C_A C_A C_A$  for the period of 4 and 5, with  $\eta = 3\pi/2$ , respectively. The results are shown in the Fig. 3(b), where the different colors correspond to different games, as displayed in the figures.

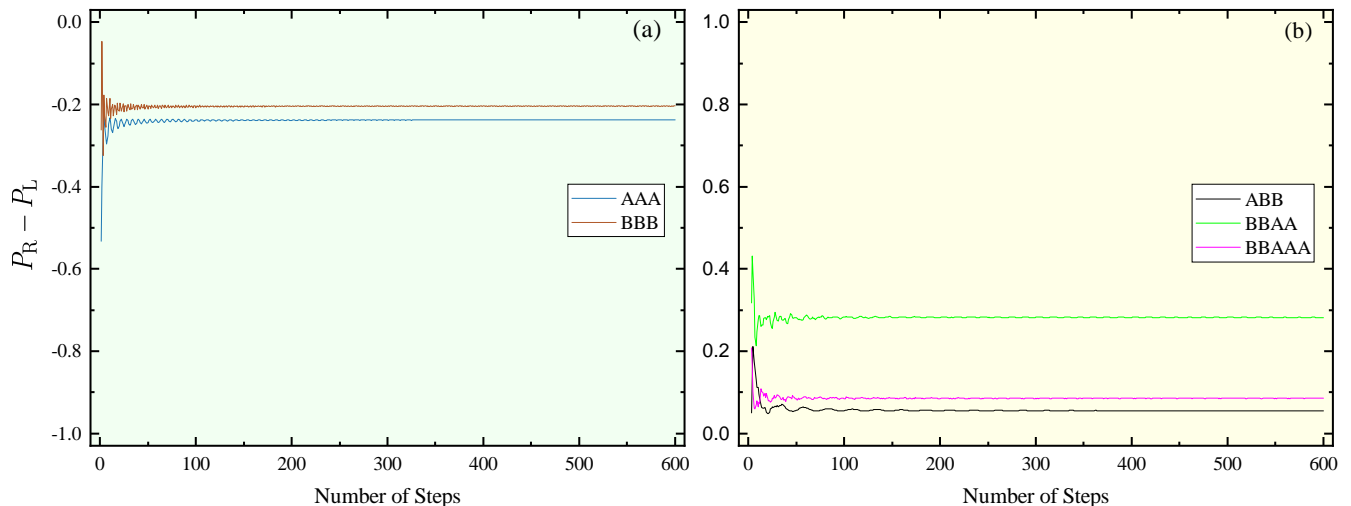


FIG. 3. (color online) Walker difference probability distribution  $P_R - P_L$  versus number of steps for (a) game A with coin operation  $C_A(150, 30, 172)$ , game B with coin operation  $C_B(175, 65, 165)$ , individually. (b) when played alternatively in particular sequences of different periods regarded as different games, e.g., game ABB with coin operation  $C_A C_B C_B$ , similarly, for BBAA, and BBAAA, with  $\eta = 3\pi/2$ . These demonstrate the occurrence of Parrondo's paradox in 1-D discrete-time QWs over infinite number of steps for coins operation  $C_A(150, 30, 172)$  and  $C_B(175, 65, 165)$ .

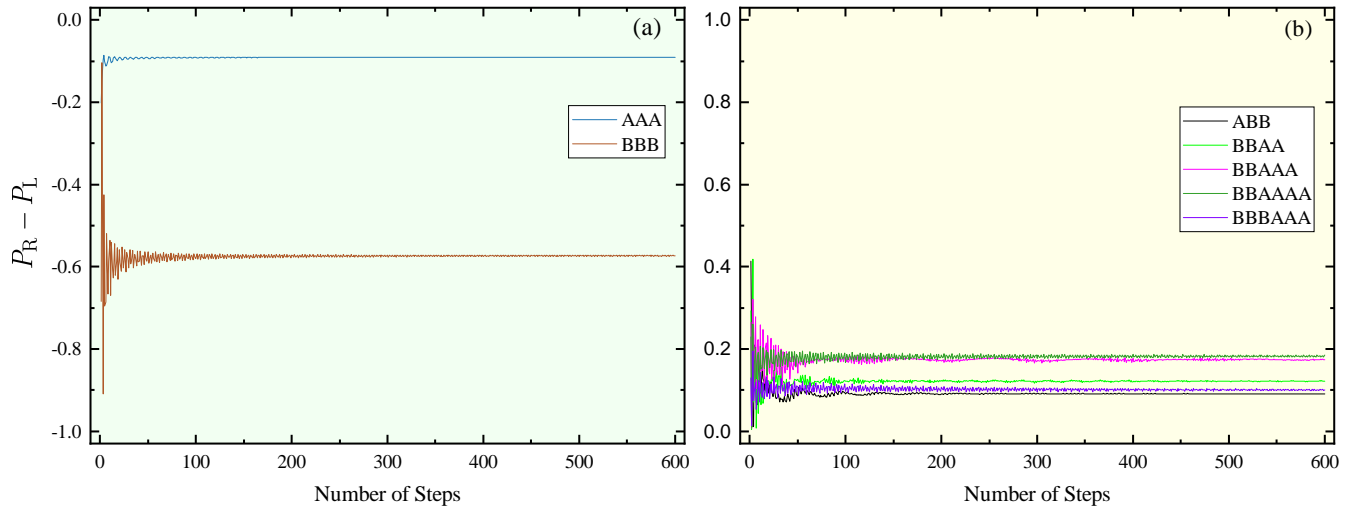


FIG. 4. (color online) Walker difference probability distribution  $P_R - P_L$  versus number of steps for (a) game A with coin operation  $C_A(155, 26, 38)$ , game B with coin operation  $C_B(170, 67, 118)$ , individually. (b) when played alternatively in particular sequences of different periods regarded as different games, e.g., game ABB with coin operation  $C_A C_B C_B$ , similarly, for BBAA, BBAAA, BBAAAA, BBBAAA, with  $\eta = 3\pi/2$ . These figures display the occurrence of Parrondo's paradox in 1-D discrete-time QWs over infinite number of steps for coins operation  $C_A(155, 26, 38)$  and  $C_B(170, 67, 118)$ .

Likewise, we also demonstrate the paradoxical behavior for the other coin parameters regime where game A with coin rotation operator  $C_A = C(155, 26, 38)$  and game B with  $C_B = C(170, 67, 118)$  for which  $P_R - P_L$  dynamics are negative throughout, representing the losing games when played individually for any time,  $t$ , as shown in Fig. 4(a). Whereas playing with both the coins simultaneously for the different sequence like, ABB, BBAA, BBAAA, BBAAAA, BBBAAA, with  $\eta = 3\pi/2$ , one can

see the dynamics of  $P_R - P_L$  that is positive throughout the time evolution, showing the paradoxical scenario, as depicted in Fig. 4(b).

Further, we discuss the scenario of the different initial state and biasing of coin parameters. In the first two cases, we have biased the coins A and B on both sides of the origin, means both  $\alpha$  and  $\gamma$ , are non-zero, representing the simultaneous biasing situation. Here, we consider the scenario of  $\gamma_A = 0$  ( $\alpha_B = 0$ ), for the

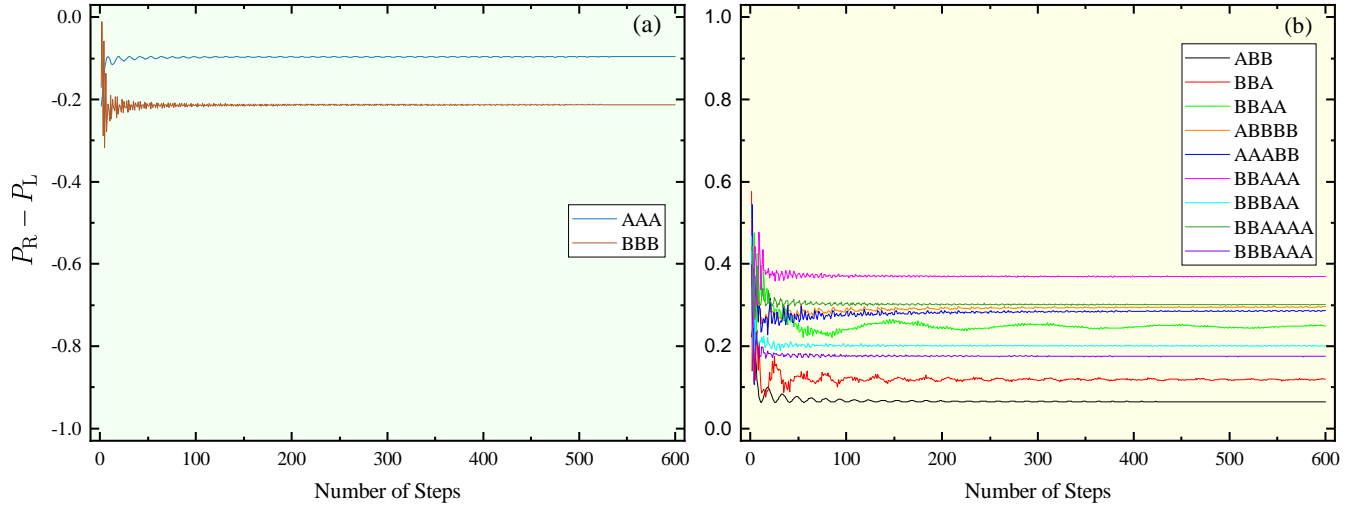


FIG. 5. (color online) Walker difference probability distribution  $P_R - P_L$  versus number of steps for (a) game A with coin operation  $C_A(156, 16, 0)$ , game B with coin operation  $C_B(0, 75, 160)$ , individually. (b) when played alternatively in particular sequences of different periods regarded as different games, e.g., game ABB with coin operation  $C_A C_B C_B$ , similarly, for BBA, BBAA, AAABB, BBAAA, BBBAA, BBAAAA, BBBAAA, BBBBAA, with  $\eta = \pi/2$ . These figure display the existence of genuine Parrondo's paradox in 1-D discrete-time QWs over infinite number of steps for coins operation  $C_A(156, 16, 0)$  and  $C_B(0, 75, 160)$ .

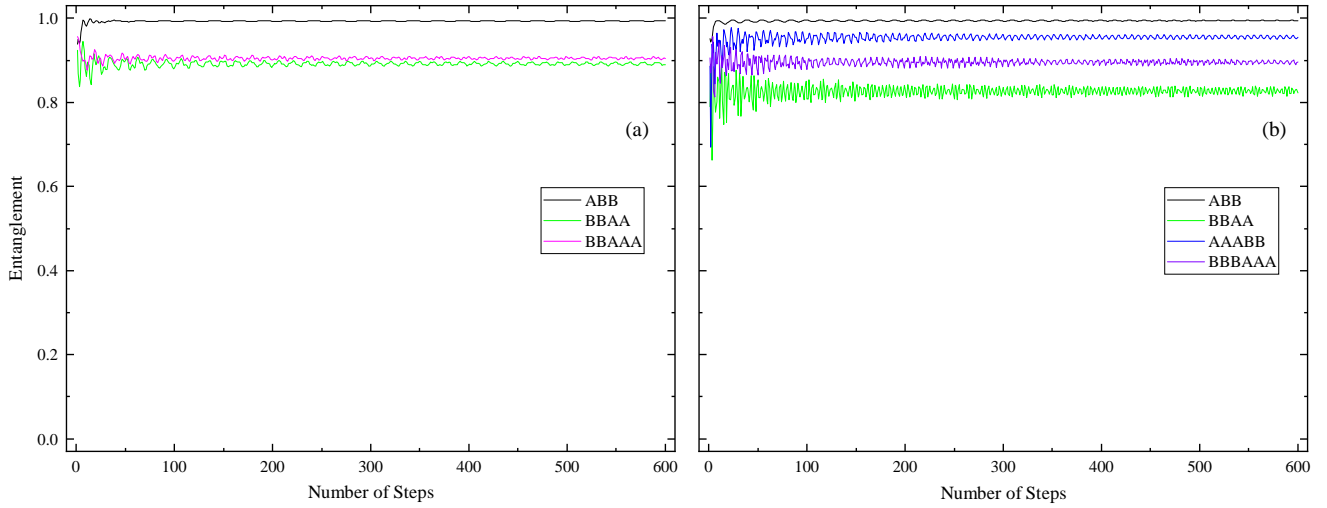


FIG. 6. (color online) Coin-position entanglement versus number of steps for coins operation (a)  $C_A(150, 30, 172)$ ,  $C_B(175, 65, 165)$ , with  $\eta = 3\pi/2$ , and (b)  $C_A(156, 16, 0)$ ,  $C_B(0, 75, 160)$ , with  $\eta = \pi/2$ , respectively.. Different colors correspond to the particular sequence of different periods, as displayed in the legends. These figures show that coin-position entanglement decreases with increasing number of periods for the corresponding coins operations.

coins A (B), respectively. Now using the coin parameters  $C_A = C(156, 16, 0)$ , and  $C_B = C(0, 75, 160)$ , we show that the game A and B are losing games when played individually for any number of steps  $t$ , as displayed in Fig. 5(a). But whenever we play alternatively with both of these coins, one can observe the paradoxical behavior for some of the particular sequence in almost every period. Limited our calculation up-to period six, we show that the sequence ABB, BBA, BBAA,

ABBBB, AAABB, BBAAA, BBBAA, BBAAAA, BB-BAAA, BBBBAA, with  $\eta = \pi/2$ , lead to a winning expectation, as shown by different colors in Fig. 5(b). Moreover, it is clear that generally, increasing the periods can enhance the outcome of the winning games, sometime even or odd period will generate maximum winning outcomes, depend strongly on the biasing parameters. According to the definition of losing and winning strategies of the Parrondo's game in the QW, we have demonstrated

that combining two losing games (A and B) in all of our three scenarios, can produce a winning game which is called Parrondo's paradox.

It may be noted that Parrondo's games are a special case of disordered QWs, which can enhance the entanglement generation between the coin and position [53, 55]. In order to calculate the coin-position entanglement numerically we use the von Neumann entropy  $S_E(\rho(t)) = -\text{Tr}[\rho_C(t) \log_2 \rho_C(t)]$ , where  $\rho_C(t) = \text{Tr}[\rho(t)]$  is the reduced density matrix of the coin and  $\rho(t) = |\Psi(t)\rangle\langle\Psi(t)|$  represents the global density matrix of the walker by assuming that the system is in a pure state. Here,  $S_E = 0$  and 1 correspond to the separable and maximally entangled states, respectively. Comparing the entanglement dynamics of Fig. 6(a) with probability distribution of Fig. 3(b), one can see that increasing period for the corresponding coin operations can enhance the asymmetry in the probability distribution of the walker toward the right of the origin, lead to a maximum winning outcome. The sequence which possesses maximum winning outcomes, e.g., BBAA in Fig. 3(b), may generate minimal entanglement than that which possesses minimal winning outcome, like ABB, generate maximal entanglement for the same coin operators. Similarly, Fig. 6(b) demonstrate the entanglement dynamics of different periods of Fig. 5(b), where one can see that the sequence ABB possesses maximum entanglement than all other sequences. In this scenario, we have also observed that the biasing of coins can also enhance the entanglement between the coin and position. From all these discussions, it becomes clear that Parrondo game is dependent on the biasing of coins and initial state, but in case of QW, the interference phenomena also play a key role in this counterintuitive behavior.

In summary, we have demonstrated the scenario of the *quantum* Parrondo effect in 1-D discrete-time QWs using different coin operators regraded as a different games. By measuring the mean position of the walker in its final step, we clearly show that two losing strategies (minus the mean position) can win by playing the two games in a particular periodic sequence, which is called Parrondo's paradox. We also discussed the coin-position entanglement generation in QWs for the same coins operation and found that the winning strategy of the period three (ABB) can generate maximal entanglement than all other sequences but the exact relations of Parrondo's games with the entanglement and coherence require further study. Furthermore, we also found that quantum interference plays an important role in such a quantum counterpart of Parrondo effect. The Parrondo's game supplies a new insight for the alternative QWS and we hope it will be helpful to develop new quantum algorithms.

This work was supported by National Key Research and Development Program of China (Nos. 2017YFA0304100, 2016YFA0302700), the National Natural Science Foundation of China (Nos. 11874343, 11474267, 11821404, 61322506, 11774335, 61725504), Key Research Program of Frontier Sciences, CAS (No. QYZDY-SSW-SLH003), Science Foundation of the CAS (No. ZDRW-XH-2019-1), the Fundamental Research Funds for the Central Universities (No. WK2470000026), the National Postdoctoral Program for Innovative Talents (No. BX201600146), China Postdoctoral Science Foundation (No. 2017M612073) and Anhui Initiative in Quantum Information Technologies (No. AHY020100, AHY060300).

### Appendix A: Analytical calculation for games A, B and ABB

The initial state of the walker, we have  $|\Psi(0)\rangle = \frac{1}{\sqrt{2}}(|0\rangle + e^{i\eta}|1\rangle)_c \otimes |0\rangle_p$ . The coins operators for the game A and B are

$$C_{A(B)} = e^{i\alpha_{A(B)}} \cos \beta_{A(B)} |0\rangle\langle 0| + e^{i\gamma_{A(B)}} \sin \beta_{A(B)} |1\rangle\langle 0| - e^{-i\gamma_{A(B)}} \sin \beta_{A(B)} |0\rangle\langle 1| + e^{-i\alpha_{A(B)}} \cos \beta_{A(B)} |1\rangle\langle 1| \quad (\text{A.1})$$

Now applying the coin operation  $C_A$  on the initial state of the walker we get,

$$[C_A \otimes \mathbb{1}] |\Psi(0)\rangle = \left( (e^{i\alpha_A} \cos \beta_A - e^{i(\eta-\gamma_A)} \sin \beta_A) |0\rangle + (e^{i\gamma_A} \sin \beta_A + e^{i(\eta-\alpha_A)} \sin \beta_A) |1\rangle \right) \otimes |0\rangle, \quad (\text{A.2})$$

after applying the shift operator, the outcome of the first step of the game A can be written as

$$|\Psi_A\rangle = S \cdot [C_A \otimes \mathbb{1}] |\Psi(0)\rangle = (e^{i\alpha_A} \cos \beta_A - e^{i(\eta-\gamma_A)} \sin \beta_A) |0\rangle \otimes |1\rangle + (e^{i\gamma_A} \sin \beta_A + e^{i(\eta-\alpha_A)} \sin \beta_A) |1\rangle \otimes |-1\rangle. \quad (\text{A.3})$$

Similarly, applying  $S \cdot [C_A \otimes \mathbb{1}]$  on Eq. (A.3), we get

$$\begin{aligned} |\Psi_{AA}\rangle = & (e^{i(2\alpha_A)} \cos^2 \beta_A - e^{i(\eta-\gamma_A+\alpha_A)} \sin \beta_A \cos \beta_A) |0\rangle \otimes |2\rangle - \\ & \sin^2 \beta_A + e^{i(\eta-\alpha_A+\gamma_A)} \cos \beta_A \sin \beta_A) |0\rangle \otimes |0\rangle + \\ & (e^{i(\alpha_A+\gamma_A)} \cos \beta_A \sin \beta_A - e^{i\eta} \sin^2 \beta_A) |1\rangle \otimes |0\rangle + \\ & (e^{i(\gamma_A-\alpha_A)} \sin \beta_A \cos \beta_A + e^{i(\eta-2\alpha_A)} \cos^2 \beta_A) |1\rangle \otimes |-2\rangle. \end{aligned} \quad (\text{A.4})$$

Again apply  $S \cdot [C_A \otimes \mathbb{1}]$  on Eq. (A.4) we approach the step three of the game A,

$$\begin{aligned}
|\Psi_{AAA}\rangle = & (e^{i(3\alpha_A)} \cos^3 \beta_B - e^{i(\eta-\gamma_A+2\alpha_A)} \sin \beta_A \cos^2 \beta_A)|0\rangle \otimes |3\rangle - \\
& (e^{i(\gamma_A-\gamma_A+\alpha_A)} \sin^2 \beta_A \cos \beta_A + e^{i(\eta-\alpha_A-\gamma_A+\alpha_A)} \cos^2 \beta_A \sin \beta_A)|0\rangle \otimes |1\rangle - \\
& (e^{i(\alpha_A+\gamma_A-\gamma_A)} \cos \beta_A \sin^2 \beta_A - e^{i(\eta-\gamma_A+\gamma_A-\gamma_A)} \sin^3 \beta_A)|0\rangle \otimes |1\rangle - \\
& (e^{i(\gamma_A-\alpha_A-\gamma_A)} \sin^2 \beta_A \cos \beta_A + e^{i(\eta-\alpha_A-\alpha_A-\gamma_A)} \cos^2 \beta_A \sin \beta_A)|0\rangle \otimes |-1\rangle + \\
& (e^{i(\alpha_A+\alpha_A+\gamma_A)} \cos^2 \beta_A \sin \beta_A - e^{i(\eta-\gamma_A+\alpha_A+\gamma_A)} \sin^2 \beta_A \cos \beta_A)|1\rangle \otimes |1\rangle - \\
& (e^{i(\gamma_A-\gamma_A+\gamma_A)} \sin^3 \beta_A + e^{i(\eta-\alpha_A-2\gamma_A)} \cos \beta_A \sin^2 \beta_A)|1\rangle \otimes |-1\rangle + \\
& (e^{i(\alpha_A+\gamma_A-\alpha_A)} \cos^2 \beta_A \sin \beta_A - e^{i(\eta-\gamma_A+\gamma_A-\alpha_A)} \sin^2 \beta_A \cos \beta_A)|1\rangle \otimes |-1\rangle + \\
& (e^{i(\gamma_A-2\alpha_A)} \sin \beta_A \cos^2 \beta_A + e^{i(\eta-3\alpha_A)} \cos \beta_A \cos^2 \beta_A)|1\rangle \otimes |-3\rangle
\end{aligned} \tag{A.5}$$

Now putting the values of coin parameters  $C_A(156, 16, 0)$  of the game A, the corresponding wave-functions takes the form

$$\Psi_A = \begin{bmatrix} 0 & 0 & -0.6210 + 0.0816i \\ 0.4714 - 0.6210i & 0 & 0 \end{bmatrix} \tag{A.6}$$

$$\Psi_{AA} = \begin{bmatrix} 0 & 0 & -0.1299 + 0.1712i & 0 & 0.5134 - 0.3144i \\ -0.6567 + 0.3610i & 0 & -0.1712 + 0.0225i & 0 & 0 \end{bmatrix} \tag{A.7}$$

$$\Psi_{AAA} = \begin{bmatrix} 0 & 0 & 0.810 - 0.0995i & 0 & 0.0944 - 0.2073i & 0 & -0.3279 + 0.4768i \\ 0.7178 - 0.0602i & 0 & 0.1233 + 0.0944i & 0 & 0.1415 - 0.0867i & 0 & 0 \end{bmatrix} \tag{A.8}$$

	$P_L$			origin	$P_R$			$\sum P_R - \sum P_L$
Positions	-3	-2	-1	0	1	2	3	
Step 1			0.6079	0	0.3923			-0.2155
Step 2		0.5616	0	0.0760	0	0.3624		-0.1992
Step 3	0.5189	0	0.0668	0	0.0794	0	0.3349	-0.1714

TABLE I. The probabilities outcomes of the game A for the first three steps of the walker.

The Tab. I shows the first three steps dynamics of the game A where one can see that the outcome  $P_R - P_L$  is throughout negative representing the losing game. Further, replacing the subscript A by B in Eq. (A.3, A.4, A.5), we can obtain the outcomes of the first three steps of game B,

$$|\Psi_B\rangle = (e^{i\alpha_B} \cos \beta_B - e^{i(\eta-\gamma_B)} \sin \beta_B)|0\rangle \otimes |1\rangle + (e^{i\gamma_B} \sin \beta_B + e^{i(\eta-\alpha_B)} \sin \beta_B)|1\rangle \otimes |-1\rangle. \tag{A.9}$$

$$\begin{aligned}
|\Psi_{BB}\rangle = & (e^{i(2\alpha_B)} \cos^2 \beta_B - e^{i(\eta-\gamma_B+\alpha_B)} \sin \beta_B \cos \beta_B)|0\rangle \otimes |2\rangle - \\
& \sin^2 \beta_B + e^{i(\eta-\alpha_B+\gamma_B)} \cos \beta_B \sin \beta_B)|0\rangle \otimes |0\rangle + \\
& (e^{i(\alpha_B+\gamma_B)} \cos \beta_B \sin \beta_B - e^{i(\eta)} \sin^2 \beta_B)|1\rangle \otimes |0\rangle + \\
& (e^{i(\gamma_B-\alpha_B)} \sin \beta_B \cos \beta_B + e^{i(\eta-2\alpha_B)} \cos^2 \beta_B)|1\rangle \otimes |-2\rangle.
\end{aligned} \tag{A.10}$$

$$\begin{aligned}
|\Psi_{\text{BBB}}\rangle = & (e^{i(3\alpha_B)} \cos^3 \beta_B - e^{i(\eta-\gamma_B+2\alpha_B)} \sin \beta_B \cos^2 \beta_B)|0\rangle \otimes |3\rangle - \\
& (e^{i(\gamma_B-\gamma_B+\alpha_B)} \sin^2 \beta_B \cos \beta_B + e^{i(\eta-\alpha_B-\gamma_B+\alpha_B)} \cos^2 \beta_B \sin \beta_B)|0\rangle \otimes |1\rangle - \\
& (e^{i(\alpha_B+\gamma_B-\gamma_B)} \cos \beta_B \sin^2 \beta_B - e^{i(\eta-\gamma_B+\gamma_B-\gamma_B)} \sin^3 \beta_B)|0\rangle \otimes |1\rangle - \\
& (e^{i(\gamma_B-\alpha_B-\gamma_B)} \sin^2 \beta_B \cos \beta_B + e^{i(\eta-\alpha_B-\alpha_B-\gamma_B)} \cos^2 \beta_B \sin \beta_B)|0\rangle \otimes |-1\rangle + \\
& (e^{i(\alpha_B+\alpha_B+\gamma_B)} \cos^2 \beta_B \sin \beta_B - e^{i(\eta-\gamma_B+\alpha_B+\gamma_B)} \sin^2 \beta_B \cos \beta_B)|1\rangle \otimes |1\rangle - \\
& (e^{i(\gamma_B-\gamma_B+\gamma_B)} \sin^3 \beta_B + e^{i(\eta-\alpha_B-2\gamma_B)} \cos \beta_B \sin^2 \beta_B)|1\rangle \otimes |-1\rangle + \\
& (e^{i(\alpha_B+\gamma_B-\alpha_B)} \cos^2 \beta_B \sin \beta_B - e^{i(\eta-\gamma_B+\gamma_B-\alpha_B)} \sin^2 \beta_B \cos \beta_B)|1\rangle \otimes |-1\rangle + \\
& (e^{i(\gamma_B-2\alpha_B)} \sin \beta_B \cos^2 \beta_B + e^{i(\eta-3\alpha_B)} \cos \beta_B \cos^2 \beta_B)|1\rangle \otimes |-3\rangle
\end{aligned} \tag{A.11}$$

Here, we put the values of coin parameters  $C_B(0, 75, 160)$  of the game B, the corresponding wave-functions takes the form

$$\Psi_B = \begin{bmatrix} 0 & 0 & -0.0506 + 0.6418i \\ -0.6418 + 0.4166i & 0 & 0 \end{bmatrix} \tag{A.12}$$

$$\Psi_{\text{BB}} = \begin{bmatrix} 0 & 0 & -0.7202 + 0.1661i & 0 & -0.0131 + 0.1661i \\ -0.1661 + 0.1078i & 0 & -0.1661 - 0.5993i & 0 & 0 \end{bmatrix} \tag{A.13}$$

$$\Psi_{\text{BBB}} = \begin{bmatrix} 0 & 0 & -0.1864 + 0.0430i & 0 & -0.1392 - 0.5558i & 0 & -0.0034 + 0.0430i \\ -0.0430 + 0.0279i & 0 & 0.5558 - 0.5438i & 0 & -0.0430 - 0.1551i & 0 & 0 \end{bmatrix} \tag{A.14}$$

	$P_L$			origin	$P_R$			$\sum P_R - \sum P_L$
Positions	-3	-2	-1	0	1	2	3	
Step 1			0.5855	0	0.4145			-0.1710
Step 2		0.0392	0	0.9330	0	0.0278		-0.0115
Step 3	0.0026	0	0.6412	0	0.3542	0	0.0019	-0.2877

TABLE II. The probabilities outcomes of the game B for the first three steps of the walker.

The Tab. II shows the first three steps dynamics of the game B where the outcome  $P_R - P_L$  is negative representing the losing game. Now playing both the games alternatively, we apply  $S \cdot [C_B \otimes \mathbb{1}]$  on Eq. (A.3),  $|\Psi_{\text{AB}}\rangle = S \cdot [C_B \otimes \mathbb{1}] |\Psi_{\text{A}}\rangle$

$$\begin{aligned}
|\Psi_{\text{AB}}\rangle = & (e^{i(\alpha_A+\alpha_B)} \cos \beta_A \cos \beta_B - e^{i(\eta-\gamma_A+\alpha_B)} \sin \beta_A \cos \beta_B)|0\rangle \otimes |2\rangle - \\
& (e^{i(\gamma_A-\gamma_B)} \sin \beta_A \sin \beta_B + e^{i(\eta-\alpha_A+\gamma_B)} \cos \beta_A \sin \beta_B)|0\rangle \otimes |0\rangle + \\
& (e^{i(\alpha_A+\gamma_B)} \cos \beta_A \sin \beta_B - e^{i(\eta-\gamma_A+\gamma_B)} \sin \beta_A \sin \beta_B)|1\rangle \otimes |0\rangle + \\
& (e^{i(\gamma_A-\alpha_B)} \sin \beta_A \cos \beta_B + e^{i(\eta-\alpha_A-\alpha_B)} \cos \beta_A \cos \beta_B)|1\rangle \otimes |-2\rangle
\end{aligned} \tag{A.15}$$

$$|\Psi_{\text{ABB}}\rangle = S [C_B \otimes \mathbb{1}] |\Psi_{\text{AB}}\rangle$$

$$\begin{aligned}
|\Psi_{\text{ABB}}\rangle = & (e^{i(\alpha_A+2\alpha_B)} \cos \beta_A \cos^2 \beta_B - e^{i(\eta-\gamma_A+2\alpha_B)} \sin \beta_A \cos^2 \beta_B)|0\rangle \otimes |3\rangle - \\
& (e^{i(\gamma_A-\gamma_B+\alpha_B)} \sin \beta_A \sin \beta_B \cos \beta_B + e^{i(\eta-\alpha_A-\gamma_B+\alpha_B)} \cos \beta_A \sin \beta_B \cos \beta_B)|0\rangle \otimes |1\rangle - \\
& (e^{i(\alpha_A+\gamma_B-\gamma_B)} \cos \beta_A \sin^2 \beta_B - e^{i(\eta-\gamma_A+\gamma_B-\gamma_B)} \sin \beta_A \sin^2 \beta_B)|0\rangle \otimes |1\rangle - \\
& (e^{i(\gamma_A-\alpha_B-\gamma_A)} \sin \beta_A \cos \beta_B \sin \beta_B + e^{i(\eta-\alpha_A-\alpha_B-\gamma_B)} \cos \beta_A \cos \beta_B \sin \beta_B)|0\rangle \otimes |-1\rangle + \\
& (e^{i(\alpha_A+\alpha_B+\gamma_B)} \cos \beta_A \cos \beta_B \sin \beta_B - e^{i(\eta-\gamma_A+\alpha_B+\gamma_B)} \sin \beta_A \cos \beta_B \sin \beta_B)|1\rangle \otimes |1\rangle - \\
& (e^{i(\gamma_A-\gamma_B+\gamma_B)} \sin \beta_A \sin^2 \beta_B + e^{i(\eta-\alpha_A-2\gamma_B)} \cos \beta_A \sin^2 \beta_B)|1\rangle \otimes |-1\rangle + \\
& (e^{i(\alpha_A+\gamma_B-\alpha_B)} \cos \beta_A \sin \beta_B \cos \beta_B - e^{i(\eta-\gamma_A+\gamma_B-\alpha_B)} \sin \beta_A \sin \beta_B \cos \beta_B)|1\rangle \otimes |-1\rangle + \\
& (e^{i(\gamma_A-2\alpha_B)} \sin \beta_A \cos^2 \beta_B + e^{i(\eta-\alpha_A-2\alpha_B)} \cos \beta_A \cos^2 \beta_B)|1\rangle \otimes |-3\rangle
\end{aligned} \tag{A.16}$$

Using both the coins operators  $C_A(156, 16, 0)$ , and  $C_B(0, 75, 160)$  simultaneously, the resultant wave function of the game ABB will be

$$\Psi_{\text{ABB}} = \begin{bmatrix} 0 & 0 & 0.1638 - 0.1056i & 0 & 0.7432 - 0.1817i & 0 & -0.0416 + 0.0055i \\ 0.0316 - 0.0416i & 0 & -0.3009 + 0.5071i & 0 & 0.1389 - 0.0723i & 0 & 0 \end{bmatrix}. \tag{A.17}$$

	$P_L$			origin	$P_R$			$\sum P_R - \sum P_L$
Positions	-3	-2	-1	0	1	2	3	
Step 1	0.0027	0	0.3857	0	0.6099	0	0.0018	0.2232

TABLE III. The probabilities outcomes of the game ABB for the first step of period three of the walker.

The Tab. III shows that the  $P_R - P_L$  dynamics of the game ABB is positive representing the winning game.

- 
- [1] J. M. R. Parrondo, "How to cheat a bad mathematician," (1996), in EEC HC&M Network on Complexity and Chaos (#ERBCHRX-CT940546), Unpublished (1996).
- [2] J. M. R. Parrondo, G. P. Harmer, and D. Abbott, *Phys. Rev. Lett.* **85**, 5226 (2000).
- [3] G. P. Harmer and D. Abbott, *Nature* **402**, 864 (1999).
- [4] G. P. Harmer and D. Abbott, *Stat. Sci.* **14**, 206 (1999).
- [5] S. Jian-Jun and W. Qi-Wen, *Sci. Rep.* **4**, 4244 (2014).
- [6] J. M. R. Parrondo and L. Dins, *Contemp. Phys.* **45**, 147 (2004).
- [7] A. Rosato, K. J. Strandburg, F. Prinz, and R. H. Swendsen, *Phys. Rev. Lett.* **58**, 1038 (1987).
- [8] H. V. Westerhoff, T. Y. Tsong, P. B. Chock, Y.-D. Chen, and R. Astumian, *Proc. Natl. Acad. Sci.* **83**, 4734 (1986).
- [9] E. Key, *Probab. Theory Relat. Fields* **75**, 97 (1987).
- [10] S. Maslov and Y.-C. Zhang, *Int. J. Theor. Appl. Finance* **1**, 377 (1998).
- [11] A. P. Flitney, J. Ng, and D. Abbott, *Physica A* **314**, 35 (2002).
- [12] C. F. Lee, N. F. Johnson, F. Rodriguez, and L. Quiroga, *Fluctuation Noise Lett.* **2**, 293 (2002).
- [13] J. Buceta, K. Lindenberg, and J. M. R. Parrondo, *Phys. Rev. Lett.* **88**, 024103 (2001).
- [14] S. Khan, M. Ramzan, and M. K. Khan, *Int. J. Theor. Phys.* **49**, 31 (2010).
- [15] S. Ethier and J. Lee, arXiv:1203.0818 [math.PR] (2012).
- [16] L. Pawela and J. Śladkowski, *Physica D* **256**, 51 (2013).
- [17] M. Pejic, arXiv:1503.08868 [math-ph] (2015).
- [18] F. A. Grünbaum and M. Pejic, *Lett. Math. Phys.* **106**, 251 (2016).
- [19] N. Masuda and N. Konno, *Eur. Phys. J. B* **40**, 313 (2004).
- [20] D. M. Wolf, V. V. Vazirani, and A. P. Arkin, *J. Theor. Biol.* **234**, 227 (2005).
- [21] F. A. Reed, *Genetics* **176**, 1923 (2007).
- [22] R. Spurgin and M. Tamarkin, *J. Behav. Finance* **6**, 15 (2005).
- [23] P. Amengual, A. Allison, R. Toral, and D. Abbott, *Proc. Royal Society London A* **460**, 2269 (2004).
- [24] F. Cannata, M. Ioffe, G. Junker, and D. Nishnianidze, *J. Phys. A: Math. Gen.* **32**, 3583 (1999).
- [25] Y. Aharonov, L. Davidovich, and N. Zagury, *Phys. Rev. A* **48**, 1687 (1993).
- [26] S. E. Venegas-Andraca, *Quantum Inf. Process* **11**, 1015 (2012).
- [27] T. D. Mackay, S. D. Bartlett, L. T. Stephenson, and B. C. Sanders, *J. Phys. A: Math. Gen.* **35**, 2745 (2002).
- [28] M. Santha, in *Theory and Applications of Models of Computation*, edited by M. Agrawal, D. Du, Z. Duan, and A. Li (Springer Berlin Heidelberg, 2008) p. 31.
- [29] R. Portugal, *Quantum Walks and Search Algorithms*, Quantum Science and Technology (Springer-Verlag New



- York, 2013).
- [30] A. M. Childs and Y. Ge, *Phys. Rev. A* **89**, 052337 (2014).
- [31] A. M. Childs, *Phys. Rev. Lett.* **102**, 180501 (2009).
- [32] A. M. Childs, D. Gosset, and Z. Webb, *Science* **339**, 791 (2013).
- [33] T. Kitagawa, M. S. Rudner, E. Berg, and E. Demler, *Phys. Rev. A* **82**, 033429 (2010).
- [34] T. Kitagawa, *Quantum Inf. Process* **11**, 1107 (2012).
- [35] T. Kitagawa, M. A. Broome, A. Fedrizzi, M. S. Rudner, E. Berg, I. Kassal, A. Aspuru-Guzik, E. Demler, and A. G. White, *Nat. Commun.* **3**, 882 (2012).
- [36] J. Eisert, M. Friesdorf, and C. Gogolin, *Nat. Phys.* **11**, 124 (2015).
- [37] J. Lang, B. Frank, and J. C. Halimeh, *Phys. Rev. Lett.* **121**, 130603 (2018).
- [38] M. Heyl, *Rep. Prog. Phys.* **81**, 054001 (2018).
- [39] X.-Y. Xu, Q.-Q. Wang, M. Heyl, J. C. Budich, W.-W. Pan, Z. Chen, M. Jan, K. Sun, J.-S. Xu, Y.-J. Han, *et al.*, arXiv:1808.03930 [quant-ph] (2018).
- [40] J. M. R. Parrondo, J. M. Horowitz, and T. Sagawa, *Nat. Phys.* **11**, 131 (2015).
- [41] S. Garnerone, *Phys. Rev. A* **86**, 032342 (2012).
- [42] A. Romanelli, *Phys. Rev. A* **85**, 012319 (2012).
- [43] A. Romanelli, R. Donangelo, R. Portugal, and F. d. L. Marquezino, *Phys. Rev. A* **90**, 022329 (2014).
- [44] A. Romanelli, *Physica A* **434**, 111 (2015).
- [45] A. P. Flitney, D. Abbott, and N. F. Johnson, *J. Phys. A: Math. Gen.* **37**, 7581 (2004).
- [46] C. Chandrashekar and S. Banerjee, *Phys. Lett. A* **375**, 1553 (2011).
- [47] A. P. Flitney, arXiv:1209.2252 [quant-ph] (2012).
- [48] M. Li, Y.-S. Zhang, and G.-C. Guo, *Fluctuation Noise Lett.* **12**, 1350024 (2013).
- [49] J. Rajendran and C. Benjamin, *EPL* **122**, 40004 (2018).
- [50] J. Rajendran and C. Benjamin, *Royal Soc. Open Sci.* **5**, 171599 (2018).
- [51] A. Schreiber, K. N. Cassemiro, V. Potoček, A. Gábris, I. Jex, and C. Silberhorn, *Phys. Rev. Lett.* **106**, 180403 (2011).
- [52] N. P. Kumar, R. Balu, R. Laflamme, and C. M. Chandrashekar, *Phys. Rev. A* **97**, 012116 (2018).
- [53] R. Vieira, E. P. M. Amorim, and G. Rigolin, *Phys. Rev. Lett.* **111**, 180503 (2013).
- [54] R. Vieira, E. P. M. Amorim, and G. Rigolin, *Phys. Rev. A* **89**, 042307 (2014).
- [55] Q.-Q. Wang, X.-Y. Xu, W.-W. Pan, K. Sun, J.-S. Xu, G. Chen, Y.-J. Han, C.-F. Li, and G.-C. Guo, *Optica* **5**, 1136 (2018).
- [56] M. Jan, Q.-Q. Wang, X.-Y. Xu, W.-W. Pan, Z. Chen, Y.-J. Han, C.-F. Li, G.-C. Guo, and D. Abbott, *Adv. Quantum Technol.* **3**, 1900127 (2020).
- [57] X.-Y. Xu, Q.-Q. Wang, W.-W. Pan, K. Sun, J.-S. Xu, G. Chen, J.-S. Tang, M. Gong, Y.-J. Han, C.-F. Li, and G.-C. Guo, *Phys. Rev. Lett.* **120**, 260501 (2018).